

Copper-catalyzed Click Chemistry for polyether-based dendronized multi-amphiphilic polymers and their applications

Shilpi Gupta*

Department of Chemistry, Hindu College, Sonipat, Haryana, India

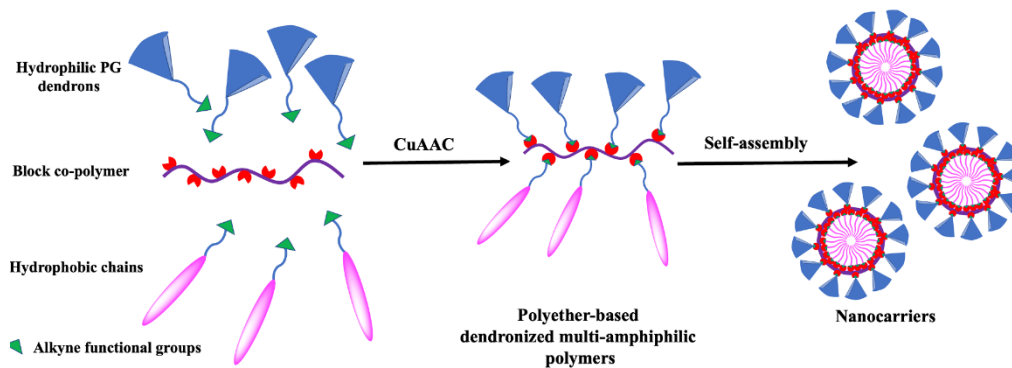
Submitted on: 02-Apr-2023, Accepted and Published on: 04-May-2023

Review

ABSTRACT

Click chemistry and bio-orthogonal chemistry stands out as dynamic tools for chemists and biologists to snap together chemical entities as well as chemical and biological building blocks with just a click to construct a variety of intricate molecular structures with ease, rapidity, and selectivity. The ground-breaking work that contributed to developing click chemistry and bio-orthogonal chemistry has been acclaimed for its biocompatibility in biological environments, high reaction rates, and simplicity. Much interest has been shown in these reactions across several disciplines, but especially in the creation of DDS and pharmaceuticals. The utilization of "click" functionalization of enzymatically synthesized polyether-based polymeric scaffolds to generate dendronized polymers and their applications in biomedicine are summarized in this mini-review article. This compilation outlines the key techniques used to click functionalize linear polymers with dendrons to create amphiphilic denpols, with a focus on drug encapsulation and delivery. Considering the findings reported from 2013 to the present, prospects of polyether-based denpols have been highlighted.

Keywords: Polyether, Novozyme-435, click chemistry, dendronized polymers, nanocarriers



INTRODUCTION

"Click chemistry" was the term first introduced by Nobel laureate K. Barry Sharpless¹ in 1999 at the 217th American Chemical Society annual conference, and it later gained popularity among the scientific community and is still the most researched chemical reaction to date and won the 2022 Nobel prize in Chemistry.^{2,3} The criteria set forth by Sharpless for reactions to be classified as "click reactions" include the chemical reaction to be modular, simple to perform, have a wide substrate scope, require mild reaction conditions, high reaction yields, easy isolation/purification of final products (preferably without chromatography), harmless or no by-products

formation, regioselective, stereospecific (may or may not be enantioselective), the ready availability of synthons/reagents and it should be possible to carry out the reaction in solvent-free environments or with solvents that are environmentally benign, like water.¹

The above criteria for a reaction being considered as a "click reaction" fit perfectly with the CuAAC reaction. The prominent name for CuAAC thus became "Click chemistry", and it is one of the most efficient, adaptable, dependable, and modular methods for the quick and regioselective preparation of 1,4-disubstituted derivatives of 1,2,3-triazole molecules. This synthetic protocol involves the addition of organic azides to terminal alkynes and is catalyzed by copper(I).⁴

With its beginning in 1893, Michael described the first 1,3-dipolar cycloaddition reaction that results in 1,2,3-triazoles by reacting organic azides with terminal alkynes.⁵ Huisgen conducted extensive additional research on the thermal 1,3-dipolar AAC reaction in the 1960s and found that it required high-temperatures of around 110°C, had slow reaction kinetics, required long reaction times and was non-regioselective giving 1,4- and 1,5-regio-isomers in equal proportions as the end products (Scheme 1).⁶⁻⁸

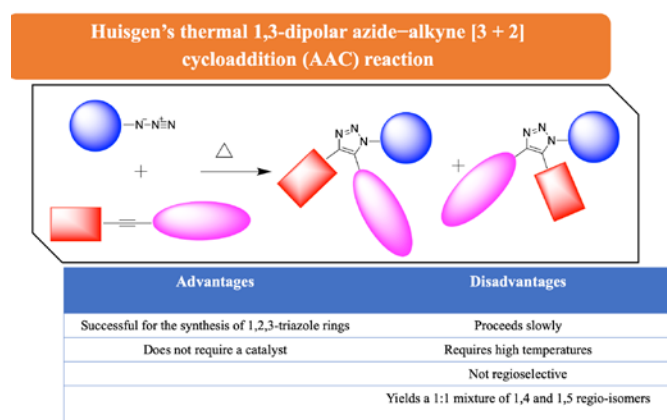
*Corresponding Author: Dr Shilpi Gupta
Department of Chemistry, Hindu College, Sonipat, Haryana-131001, India

Tel: +91 9868427037
Email: drshilpigupta.chem@gmail.com



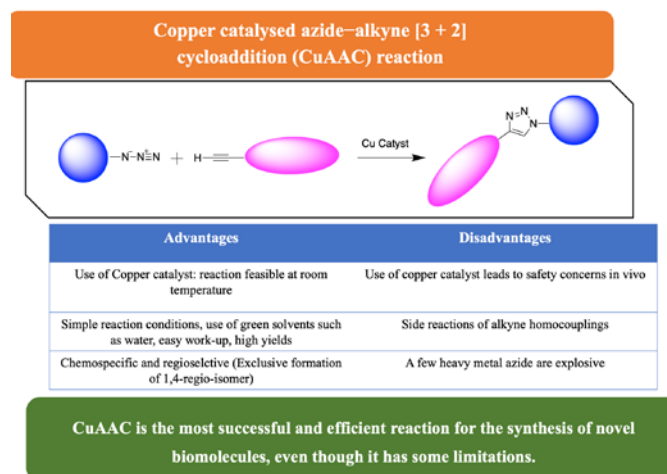
URN:NBN:sciencein.jmc.2023.583.
© ScienceIn Publishing
<https://pubs.thesciencein.org/jmc>





Scheme 1. Huisgen's thermal AAC reaction and its merits and demerits.

The modified form of this reaction, which was conducted at room temperature using a copper catalyst, was separately and independently reported by Sharpless⁹ and Meldal¹⁰ in 2002. It was found that using a Cu(I) catalyst causes the reaction to exclusively produce the 1,4-regioisomer, significantly speeds up the reaction rate (second-order rate constant, $k = 10\text{--}100 \text{ M}^{-1}\text{s}^{-1}$ with $20 \mu\text{M}$ Cu(I)) and removes the need for high temperatures (Scheme 2). The Cu(I) catalyst reduces the activation energy barrier for the generation of the triazole ring, leading to dramatically improved kinetics and a high second-order rate constant.^{9–12} Many procedures have been established to use Cu as a catalyst for CuAAC.¹³ The three main strategies include either the use of Cu(I) salts directly,¹⁴ or oxidation of Cu(0);¹⁵ or conversion of Cu(II) salts into the active catalyst by the addition of reducing agents such as sodium ascorbate etc.¹¹

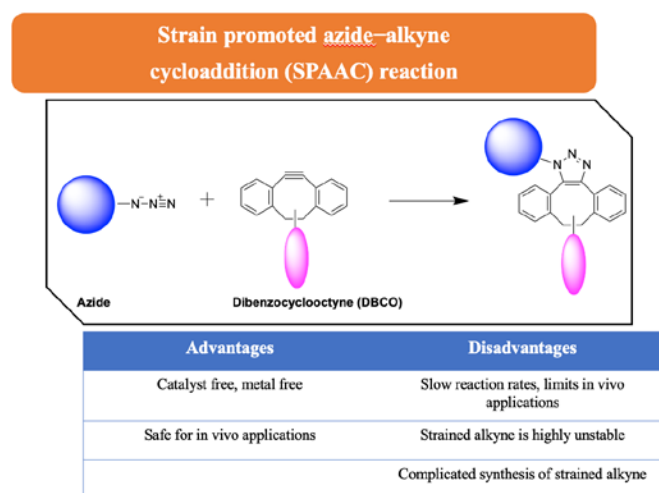


Scheme 2. CuAAC reaction and its merits and demerits.

The reaction thus can be performed with readily available azides and terminal alkynes, is simple and modular way, has a broad substrate scope, provides very good yields, gives no by-products, is highly regioselective, stereospecific and feasible in environmentally benign solvents like water under mild reaction conditions. However, the inclusion of a cytotoxic copper catalyst raised some issues with this adaptable reaction, limiting its utility *in vitro* and *in vivo* applications. Despite this, it has

been described as the most effective and successful "click reaction" to date, and it has been discussed in several recently published review articles.^{4,12,16–18}

Further research to eliminate the use of cytotoxic metal catalysts led to the development of SPAAC reactions, where the alkynes were used as a part of strained ring systems such as cyclooctyne (Scheme 3).¹⁹ However, the reaction kinetics was found to be much slower than the CuAAC, which led to the generation of modified strained alkynes such as cyclooctyne bearing fluorine atoms,²⁰ incorporation of sp^2 hybridized carbons in cyclooctyne rings,²¹ cyclopropane rings fused to cyclooctyne,²² and other strained systems such as DIFO,²⁰ BARAC,²³ TMTH²⁴ etc. Although the metal-free click reaction with moderate second-order reaction rates ($1\text{--}60 \text{ M}^{-1}\text{s}^{-1}$) has been achieved by SPAAC, still a serious limitation arises from the use of large strained ring structures of alkynes, which are not just difficult to synthesize but also curtails its use in different synthetic applications, especially in polymer chemistry.²⁵ However, SPAAC has gained a lot of attention as the metal-free alternative to copper-catalyzed click reactions and offers a variety of applications.²⁶



Scheme 3. SPAAC reaction and its merits and demerits.

Although further discussion is beyond the purview of this mini-review, recently published articles^{27–29} and reviews^{4,16–18,26,30–36} highlight the numerous additional alterations and adaptability of click chemistry in detail.

Polyether-based scaffolds

Polyether-based scaffolds have drawn a lot of interest among the numerous drug-delivery systems investigated.^{37–42} Due to their great biocompatibility, hydrophilic polyether-based polymers are frequently utilised to improve the pharmacokinetic characteristics of drug carriers. PEG is regarded as the benchmark standard for drug delivery and has received FDA approval for a variety of pharmaceuticals.^{38,39} It has prospective uses in the biomedical and pharmaceutical industries due to its unique qualities, which include chemical non-reactivity, solubility in aqueous media, well-established safety profile, reduced contact with blood, and biocompatibility.⁴⁰

Additionally, polyols with an aliphatic dendritic polyether scaffold, with the possibility of multiple groups on the architectural periphery for functionalization, and a closely-packed, perfectly structured tree-like dendritic structure have grown in significance.^{40–45} For example, OG and PG have outstanding characteristics such as numerous hydrophilic end-groups, and flexible and highly biocompatible polyether architecture.^{41,42,45} These substances have the ability to alter the therapeutic efficacy of the active molecules. Numerous studies have been reported using these versatile polyether scaffolds for drug-delivery applications using click chemistry as an indispensable tool for the attachment of drugs, dyes and molecular probes.^{40–45}

Dendronized Polymers

Block copolymers' design and synthesis have drawn a great deal of interest since they serve as the framework for materials that can be used for a variety of purposes.⁴⁶ Dendronized polymers (more commonly known as denpols), which have been the focus of intensive research over the past two decades, were introduced as a new branch in the field of block copolymer synthesis, primarily for their applications at nanoscale levels.^{47,48} Denpols are highly intriguing because of the intrinsic topological differences between the linear and dendritic segments and the adjustable amphiphilicity that allows them to self-assemble into nanostructures with unusual morphologies.⁴⁹ Their distinctive framework is advantageous over spherically shaped dendrimers in particular for nanoscale applications where the classical dendrimers' spherical shape may make them inappropriate for use.^{50,51} Similar in nature (but not in architecture) to the spherically shaped dendrimers, these denpols can be customized appropriately with precise structure, different molecular dimensions and shapes, rigidity at a higher degree of dendronization,^{52–55} plus having multiple options for surface functionalization while retaining the properties of the linear backbone.^{50,51,56,57} In view of these characteristics they may adopt cylindrical shapes⁵⁸ and thus have appropriately been referred to as “molecular cylinders”.⁴⁷

There are three primary methods for the generation of denpols as depicted in Figure 1. Method 1 involves the attachment of a preconstructed dendron to a polymer backbone that has suspended functional groups using a “graft to” technique (Figure 1a).^{59–62} Convergent synthesis makes this technique appealing, however full coverage of the backbone employing high-generation dendrons (G3 or larger) is a difficult task.⁶³ Method 2 is a “graft from” approach (Figure 1b), which proceeds from the polymer backbone through a step-growth process.⁶⁴ Although the possibility of structural flaws makes this pathway seem difficult, it still offers a technique to attain the highest level of dendronization.⁶⁵ Recently, Fytas and Choi *et al.*, reported the successful synthesis of up to sixth-generation denpols *via* this method using ROMP.⁶⁶ Dendrons are incorporated into the monomer in Method III, the “macromonomer” strategy (Figure 1c). The polymer's repeat units all have flawless pre-attached pendant dendrons, which is advantageous, and the highest dendronization is possible with

this method.^{67–69} The drawback with this synthetic strategy is that it typically only achieves low degrees of polymerization due to high steric strain.⁷⁰ These macromonomers can only be polymerized using standard homopolymerization techniques such as step growth⁷¹ or radical chain growth mechanisms.^{68,72} To achieve this, a variety of techniques have been used, including radical,⁷³ living cationic,^{74,75} ATRP,⁷⁶ ROMP,^{77,78} Suzuki,⁷⁹ and Heck coupling.⁸⁰

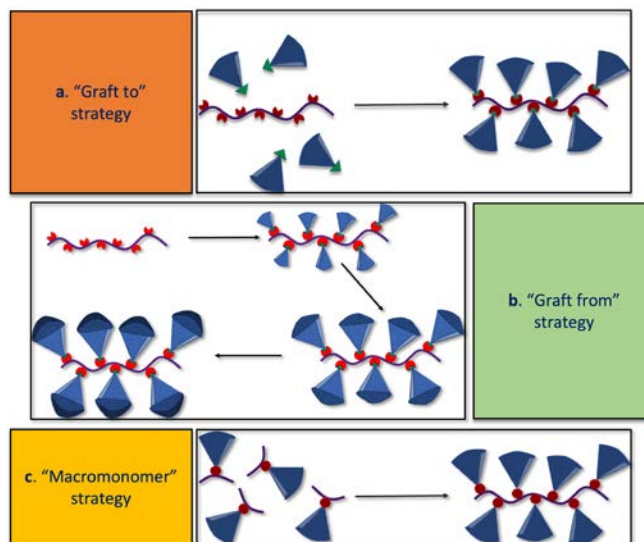


Figure 1. Different strategies for the generation of denpols; **a)** the “Graft to” approach, **b)** the “Graft from” approach and **c)** the “Macromonomer” approach.

Not just chemical synthesis but the biocatalytic “green” approach is an alternative for producing multifunctional polymers with fine composition and an established structure, polymerization employing enzymes as biocatalysts have gained popularity.^{81–85} Lipases (hydrolytic enzymes), one of the several classes of known enzymes, have garnered a great deal of attention lately. Lipases (EC 3.1.1.3) are omnipresent in most living species. The synthesis or cleavage of ester linkages in triacylglycerols is a natural function of lipases. They are the most adaptable group of enzymes due to their attributes such as steadiness in organic solvents, high catalytic performance absent cofactors, wide specificity of the substances on which it acts, and excellent chemo-, regio-, and stereo-selectivity.^{81,86,87} Recent reviews have highlighted the application of lipases in the synthetic transformation of small molecules as well as the development of polymeric systems for drug delivery applications.^{81–88}

Considering the significance of polyether scaffolds and amphiphiles based on polyethers for DDS, this mini-review emphasises the versatility of the CuAAC as an effective method for the functionalization of enzymatically synthesised linear polyether-based copolymers to generate a variety of oligo glycerol-dendronized multi-amphiphilic polymers by “graft to” method.

CUAAC FOR THE SYNTHESIS OF POLYETHER-BASED DENDRONIZED MULTI-AMPHIPHILIC POLYMERS

N435 catalyzed block copolymers

Parmar and co-workers explored the field of lipase-catalyzed synthesis of PEG-based macromolecular systems utilizing pharmaceutically notable small molecules like polyphenols, amides, nucleosides, etc., and their uses as carriers for drugs and genes.⁸¹ On the other hand, Haag and colleagues investigated dendritic PGs for biological and pharmaceutical applications.^{41,43,44,89}

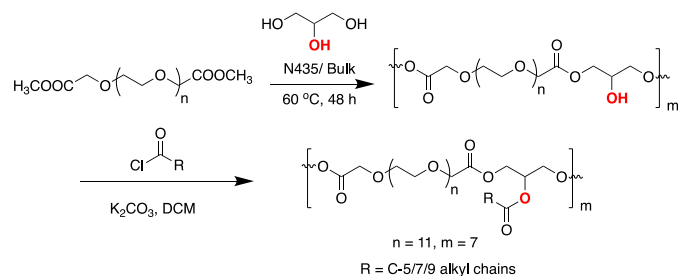
Further work by Sharma and co-workers explored a new area utilizing lipases for catalytic step-growth condensation polymerization of glycerol/glycerol derivatives (azido-glycerol/azido-tri-glycerol) and PEG-based linear block copolymers. With the advancement in these block copolymers, dendronization with oligo glycerol (polyether dendrons) was carried out using highly efficient CuAAC reactions and different series of denpols were generated, which are going to be discussed in the following sections.

N435 catalyzed PEG₆₀₀-co-glycerol polymers (Block copolymer 1)

Regioselective synthesis of PEG₆₀₀-co-glycerol block copolymer was carried out by N435 (an immobilized enzyme) catalyzed transesterification polymerization of PEG₆₀₀bis(carboxymethyl)ether dimethyl ester with primary hydroxyl groups of glycerol (Scheme 4).⁹⁰

Acylation with C-5, C-7 and C-9 acyl chains

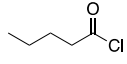
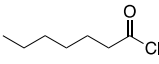
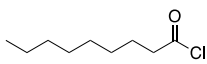
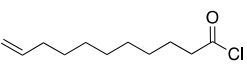
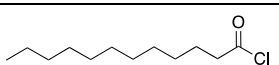
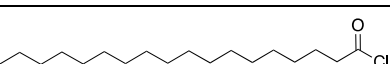
The post-functionalization of the linear copolymer was done with hydrophobic acyl chains of different chain lengths i.e. C-5, C-7 and C-9 acyl chlorides (Table 1) *via* an acylation process onto the pendant secondary hydroxyl groups of glycerol moieties (Scheme 4, Table 5, entry 1.1).⁹⁰ In aqueous media, the polymers created amphiphilic micellar aggregates, as observed by SLS techniques. The nanocarriers were further assessed for encapsulation of the hydrophobic drug vitamin E.⁹⁰



Scheme 4. Synthesis of PEG₆₀₀-co-glycerol polymers and their acylation with different acyl chlorides (Table 1) to generate polymeric nanocarriers.⁹⁰

This synthetic strategy created nano-architectures with fine-tuneable hydrophobic segments, however, the limitation of the pendant hydroxyl group is that complete functionalization is difficult to achieve and further fine-tuning of the hydrophobic-hydrophilic balance by attaching hydrophilic groups like OG/PG dendrons may have limited attachments through traditional chemical coupling methods.

Table 1. Hydrophobic acyl chlorides used for acylation in Schemes 4 and 6.

Hydrophobic R' groups
 C-5 acyl chloride (C ₄ H ₉ COCl)
 C-7 acyl chloride (C ₆ H ₁₃ COCl)
 C-9 acyl chloride (C ₈ H ₁₇ COCl)
 C-11 terminal alkenoyl chloride (C ₁₀ H ₁₉ COCl)
 C-12 acyl chloride (C ₁₁ H ₂₃ COCl)
 C-18 acyl chloride (C ₁₇ H ₃₅ COCl)

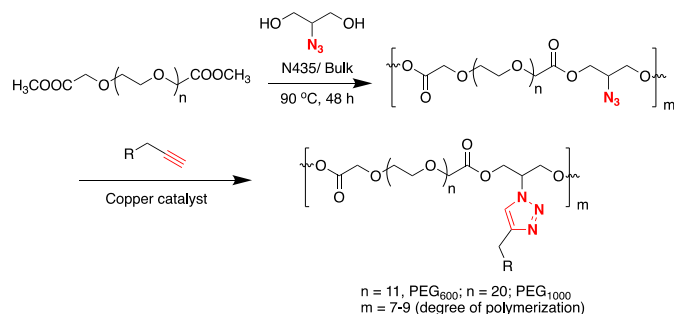
N435 catalyzed PEG₆₀₀-co-azido-glycerol polymers (Block copolymer 2)

Exploring the chemistry for efficient functionalization and bio-orthogonal approach, Sharma and co-workers developed a novel class of polyether-based denpols by collaborating with Haag and colleagues to effectively functionalize these polymeric systems utilizing OG/PG dendrons as side chains *via* highly efficient CuAAC using the “graft to” strategy (Figure 1a). A new class of multi-amphiphilic polyether-based denpols⁹¹ were designed by selectively functionalizing glycerol to azido-glycerol by N435 catalyzed reaction (protection of primary hydroxyl groups of glycerol, followed by azidation and deprotection of hydroxyl groups) and then transesterification polymerization of PEG₆₀₀bis(carboxymethyl)ether dimethyl ester with azido-glycerol's hydroxyl groups by the previously reported protocol⁹⁰ (Scheme 5).

Click functionalization with OG dendrons ([G1.0] and [G2.0]) and hydrophobic chains (C-18)

The PEG₆₀₀-co-azido-glycerol polymers (Scheme 5) enabled efficient CuAAC reactions *via* pendant azide functionality on the copolymer backbone with alkyne functionalized C-18 hydrophobic chains (Table 2) and [G1.0] and [G2.0]-OG dendrons as hydrophilic side chain appendages (Table 3) in different ratios to fine-tune the hydrophobic-hydrophilic balance (Table 5, entry 2.1).⁹¹

In aqueous media, the rearrangement of the exterior surface with hydrophilic dendrons and the interior core with hydrophobic alkyl chains created micelles (Figure 2) with



Scheme 5. Synthesis of PEG-co-azido-glycerol polymers and their click functionalization with various hydrophobic (**Table 2**) and/or hydrophilic R groups (**Table 3**) to generate non-dendronized / dendronized polymers.

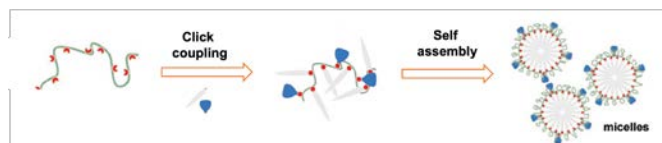


Figure 2. Schematic representation of (PEG₆₀₀-co-azido glycerol) polymers synthesis and their functionalization to self-assembled nano-micellar architectures. Reprinted from reference⁹¹ copyright (2013) WILEY-VCH Verlag GmbH & Co. KGaA, Weinheim.

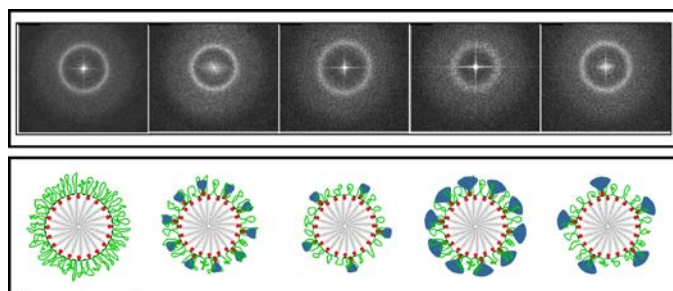


Figure 3. Comparison of the five FT of cryo-TEM images with five graphical models for the non-dendronized (1st) and the dendronized multi-amphiphilic polymers' (2nd – 5th) spatial micellar structure. The addendum proportions and the dendron generations influence the micellar dimensions and exterior patterns. Reprinted from reference⁹¹. Copyright (2013) WILEY-VCH Verlag GmbH & Co. KGaA, Weinheim.

diameters in the nanometer range and CAC values in the micromolar range (Table 5, entry 2.1). The FT of cryo-TEM images observed experimentally were compared with models created by graphical modelling (Figure 3). Both depict the effect of dendron generation and addendum proportion (both hydrophilic and hydrophobic) on the micellar dimensions and exterior patterns (Figure 3).⁹¹

In addition to assisting in preserving the amphiphilicity of micellar structures, OG dendrons also improved the robustness, biocompatibility, and transport capacity of the newly synthesized micellar denpols. These micelles' potential to serve as nanocarriers for drug transport systems was demonstrated with hydrophobic pyrene as a guest molecule and binding investigations with fluorescent dye 1-anilinonaphthalene-8-sulfonic acid (ANS) utilizing spectrofluorometric techniques revealed unimolecular binding properties in the micelle's hydrophobic domain, indicating that the guest molecules are primarily found inside the aggregates' hydrophobic cores.⁹¹ The

higher guest solubilization efficiency, increased biocompatibility using polyether-based PEG and OGs and reduced exchange rates due to covalently linked amphiphiles as compared to unimolecular amphiphiles encouraged further research for more stable architectures to acquire controlled drug release capabilities by fine-tuning the structure of the denpols.

Table 2. Hydrophobic R groups used for click functionalization in Schemes 5 and 6.

Hydrophobic R groups
 C-18 (~OC ₁₈ H ₃₇)
 C-14 (~C ₁₁ H ₂₃)
 C-12 (~C ₉ H ₁₉)
 C-8 (~OC ₈ H ₁₇)
 Fluoro-C-8 (~OC ₈ H ₄ F ₁₃)
 Azobenzene (~OC ₁₆ H ₁₇ N ₂)

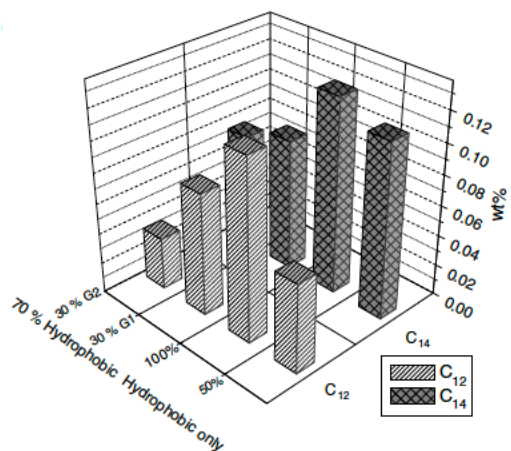
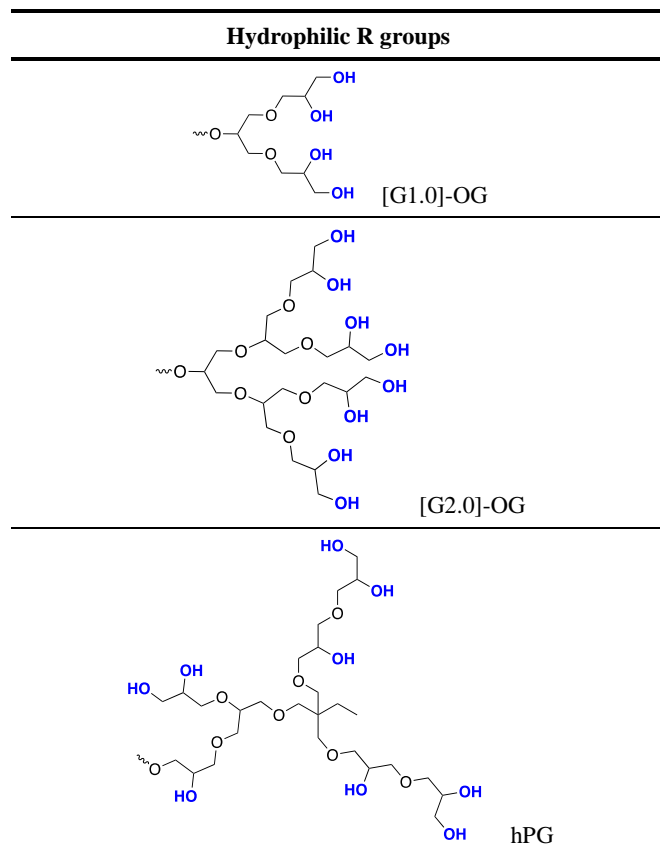
N435 catalyzed PEG₁₀₀₀-co-azido-glycerol polymers (Block copolymer 3)

Kumari *et al.*, later explored the influence of PEG chain length on supramolecular self-assembly and the physiochemical characteristics of this novel class of denpols by substituting a longer PEG₁₀₀₀ chain for PEG₆₀₀ (Scheme 5).⁹²

Click functionalization with OG dendrons ([G1.0] and [G2.0]) and hydrophobic chains (C-12 and C-14)

The hydrophobic tails (C-12 and C-14, Table 2) and the hydrophilic dendrons ([G1.0] and [G2.0]-OG, Table 3) were subsequently appended to the linear block PEG₁₀₀₀-co-azido-glycerol polymers using an effective copper-catalyzed "Click chemistry" (Scheme 5, Table 5, entry 3.1).⁹²

The resulting amphiphilic denpols in an aqueous solution self-assembled to generate distinct micelles. To study the transport behaviour of these polymers, Nile red was used as a fluorescent model dye. A few exemplary polymers' cytotoxicity profiles and biocompatibility were investigated in connection with the attachment of hydrophilic oligo glycerol dendrons and the length of hydrophobic alkyl chains. In comparison to their C-12 counterparts, the C-14 alkyl chain-attached non-dendronized polymers exhibited a better transport capacity.

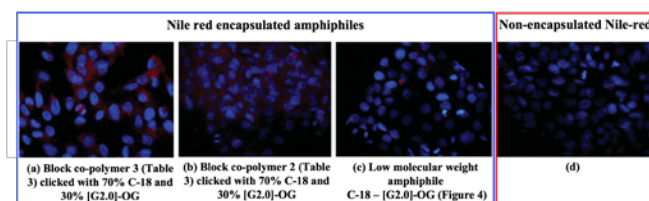
Table 3. Hydrophilic R groups used for click functionalization in Scheme 5 and 6.**Figure 4.** The transport capacity of Nile red encapsulated non-dendronized/dendronized polymers. Reproduced from reference ⁹². Copyright 2014 John Wiley & Sons, Ltd.

Besides that, the transport capacity was reduced when OG dendrons were grafted to create denpols (Figure 4), however, the biocompatibility of the denpols was found to be better than the non-dendronized counterparts.⁹² This study moved a step ahead in the search for fine-tuning the amphiphilic architecture and obtaining more biocompatible denpols.

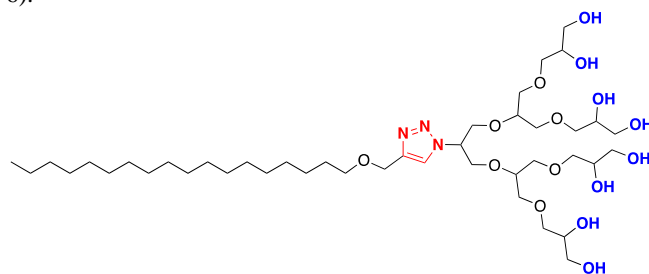
Click functionalization with OG/PG dendrons ([G1.0], [G2.0] and hPG) and hydrophobic chains (C-18)

In a similar set of nano-micellar denpols with PEG₁₀₀₀ as monomers, an extra hPG (Table 3) as a hydrophilic addendum

via “click chemistry” was also explored for their transport behaviour and other properties (Table 5, entry 3.2).⁹³ The transport efficiency of the Nile red encapsulated non-dendronized, as well as dendronized polymers, were evaluated, and found to be maximum (4.60 mg/g) for 50% C-18 and 50% [G2.0]-OG grafted denpol, followed by the 70-50% C-18 and 30-50% hPG grafted denpols (2.73, 2.71 mg/g respectively).⁹³ Photographs of QGP-1 cells treated with denpols encapsulating the dye Nile red (Figure 5a), showed improved dye uptake using FACS analysis and cellular fluorescence microscopy compared to (i) dye-loaded PEG₆₀₀ counterpart denpols (Figure 5b), (ii) [G2.0]-OG dendron - C-18 alkyl chain ‘clicked’ amphiphile (Figure 5c and 6) and (iii) free dye Nile red (Figure 5d).⁹³

**Figure 5.** Fluorescence pictures of QGP-1 cells with red coloured Nile red and blue-stained DAPI nuclei for (a) PEG₁₀₀₀ and (b) PEG₆₀₀-based denpols, (c) C-18 – [G2.0]-OG amphiphile and (d) non-encapsulated Nile red (blank cells). Reproduced from reference ⁹³. Copyright 2015 Wiley-VCH Verlag GmbH & Co. KGaA.

Furthermore, even at concentrations as high as 500 (μg/mL), these micelles exhibited little cytotoxicity after 72 hours. The improved intracellular stability of supramolecular self-assembled denpols could explain why polymeric amphiphiles have a better transport potential than small amphiphiles (Figure 6).

**Figure 6.** C-18 – [G2.0]-OG ‘clicked’ amphiphile.

The work however concluded the need for longer alkyl chains for the effective encapsulation of hydrophobic pharmaceuticals and the importance of maintaining a balance between hydrophilic and hydrophobic scaffolds to preserve biocompatibility.⁹³ With the purpose of creating the best possible drug/dye delivery systems, more modifications were needed to better understand the encapsulation phenomena.

Click functionalization with OG dendrons ([G2.0]) and hydrophobic chains (azobenzenes)

The photoresponsive behaviour of azobenzene moiety is well known in the literature as an essential component for the development and breakdown of supramolecular structures.^{94–97} Also click chemistry has been a mainstay option for the conjugation of azobenzene within the polymer's main chain⁹⁵ or

grafted to the polymers as side appendages.⁹⁶ Yet, due to their distinct characteristics, polymers with pendant azobenzenes have garnered much consideration,⁹⁷ as opposed to the polymers containing azobenzenes in the main chain. Such polymers have the added benefit of exhibiting photoresponsivity even at lower azobenzene proportions as the block copolymers' segregation capacity improves because of nanoscale interactions between different azobenzene moieties, which produce well-defined structures. To introduce this photoresponsive behaviour in the amphiphilic nano-carriers, Kumari *et al.*, generated photoresponsive non-dendronized polymers as well as denpols (Scheme 5) by grafting azobenzenes (Table 2) and/or [G2.0]-OG dendrons (Table 3) on PEG₁₀₀₀-*co*-azido-glycerol base copolymer using "click" functionalization (Table 5, entry 3.3).⁹⁸ In the aqueous solution, supramolecular aggregation behaviour was displayed by both non-dendronized as well as dendronized polymers with azobenzene in the side chain as observed *via* DLS and cryo-TEM measurements (Figure 7).

Curcumin and Nile red were used to investigate the encapsulation capability of polymeric systems. Curcumin encapsulation was studied qualitatively, due to the superimposition of the curcumin and polymers' absorption spectra, while Nile red at a concentration of 0.4 mM per mg per ml of the polymer's solutions was quantitatively investigated. When compared to the non-dendronized analogue (70% azobenzene grafting only), the dendronized polymer (70% azobenzene and 30% [G2.0]-OG grafting) demonstrates superior transport potential with encapsulation efficiencies of 1.45 and 1.87%, respectively. When compared to earlier synthesized similar denpols with C-12 and C-14 alkyl chains and [G2.0]-OG grafting (Table 5, entry 3.1), the transport efficiency of these azobenzene grafted denpols was found to be 7 and 3 times significantly higher, respectively.⁹² Plausible explanation for azobenzene functionalized denpols' higher encapsulation potential could be explained by the interactions between the π -electron cloud of azobenzene's aromatic rings with the ones in Nile red, both inside the hydrophobic nanomicellar core.

UV-vis spectroscopy was used to investigate the photoisomerization of the polymers. The release profile of the polymers encapsulating Nile red was affected by isomerization. It was observed that photoisomerization (*cis-trans* and *trans-cis*) takes place at a faster pace at concentrations below CAC than at concentrations above CAC. Azobenzene-grafted non-dendronized polymers showed a higher discharge of Nile red as compared to the azobenzene and [G2.0]-OG grafted denpols, demonstrating the denpols ability to form stable micelles. The intensity of Nile red fluorescence decreased because of the *trans-cis* isomerization, while vice-versa was observed for *cis-trans* isomerization. On one entire *trans-cis-trans* photoisomerization cycle, the intensity of Nile red fluorescence could not be fully recovered, indicating some net dye release. These results suggest that the azobenzene moieties mediate the photoresponsive release and that [G2.0]-OG dendrons increase the stability of the formed micelles and their potential for encapsulation.

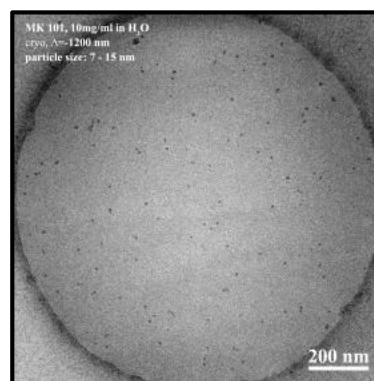


Figure 7. Spherical micelles with diameters ranging from 7 to 15 nm displayed by cryo-TEM measurement of the 70% azobenzene-grafted non-dendronized polymers. Reproduced from reference ⁹⁸. Copyright 2015 Royal Society of Chemistry.

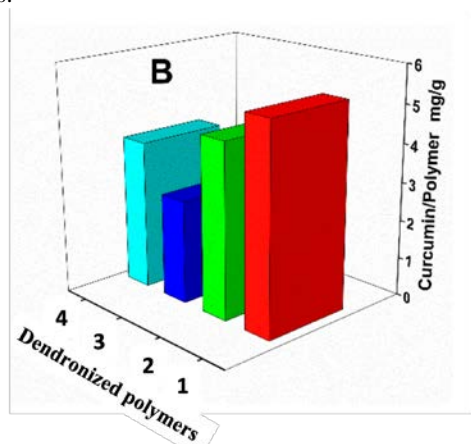
Click functionalization with OG dendrons ([G2.0]) and hydrophobic chains (C-8 and fluoro C-8)

In another study by Parshad *et al.*, hydrophobic fluorinated alkyl tails were used to further modify the hydrophobic-hydrophilic balance of denpols (Scheme 5). It is well known that compared to the electron cloud surrounding hydrogen in alkyl chains, the electron cloud surrounding fluorine atoms in fluoroalkyl analogues is relatively more tightly held, and due to that the polarization is much reduced, thus replacing the alkyl tails with their fluorinated versions leads to diminished unwanted interactions among the pendant hydrophobic chains.^{99,100} Further, the higher surface area of the fluorine atoms than the hydrogen atoms increases the overall hydrophobic character of perfluoroalkyl chains,^{101,102} and would thus enable the formation of stiffer and neatly packed stable micellar aggregates with CMC values in micromolar range, suggesting that they would be more effective for applications in drug delivery.

Keeping in view these facts, PEG₁₀₀₀-*co*-azido-glycerol (Scheme 5) was appended with hydrophobic fluoro C-8 chains or C-8 alkyl chains (Table 2) and hydrophilic [G2.0]-OG dendrons (Table 3) using highly efficient copper-catalyzed click chemistry (Table 5, entry 3.4) to generate a new series of denpols.¹⁰³ Using the hydrophobic drugs curcumin and dexamethasone, the resultant polymers were then evaluated for their self-assembly behaviour, the extent of hydrophobic drug solubilization, transport potential, and drug release profiles.

DLS and *cryo*-TEM measurements revealed smaller micellar dimensions (8-10 nm) for the perfluoroalkyl chain appended denpols compared to larger micelles (100-150 nm) formed by the alkyl grafted denpols. The transport potential of denpols was quantified by studying the absorption spectra of the denpols encapsulating curcumin (Figure 8). Denpols with fluoro C-8 chain and [G2.0]-OG dendron (denpol 1- 70% fluoro C-8 and 30% [G2.0]-OG grafting and denpol 2- 50% fluoro C-8 and 50% [G2.0]-OG grafting) had the highest level of curcumin encapsulation, with transport efficiencies of 5.3 and 4.5 mg drug/g denpol, respectively. However, denpols 3 and 4 (C-8 alkyl analogues of denpols 1 and 2), had quantitatively less drug transport efficiencies, respectively (Figure 8). A similar trend

was observed for the encapsulation of the highly hydrophobic fluorinated steroidal drug dexamethasone. Perfluoro-grafted denpols exhibited greater transport efficiencies for this drug as well, which may be explained by their stable multi-amphiphilic micellar structures, which are the result of the orderly packing of perfluoroalkyl chains in the hydrophobic core of the micelles.¹⁰³



Dendronized polymers	Hydrophobic content	Hydrophilic content
1	70% fluoro C-8 chain	30 % [G2.0]-OG
2	50% fluoro C-8 chain	50 % [G2.0]-OG
3	70% C-8 alkyl chain	30 % [G2.0]-OG
4	50% C-8 alkyl chain	50 % [G2.0]-OG

Figure 8. Transport efficiency of perfluoro alkyl chain grafted denpols compared to alkyl chain grafted denpols for hydrophobic drug curcumin in mg/g. Reproduced from reference ¹⁰³. CC4.0.

Along with drug encapsulation, the enzyme-triggered controlled drug release also plays a crucial role to maintain the therapeutic concentrations under physiological conditions. Thus, N435-mediated release of the hydrophobic drug curcumin was investigated by incubating the drug-encapsulated nanocarriers with the enzymes in the dark. Figure 9 depicts a proposed drug release from amphiphilic polymers.¹⁰³ In order to conduct a comparative release study, N435 (200 wt%) was added to the curcumin-encapsulated denpols solution (fluorinated and alkyl analogues). Both fluorinated and non-fluorinated denpols showed up to 90% curcumin release triggered by the enzyme within 12 days; however, fluorinated denpols showed a faster release, which was presumed to be due to their enhanced fit with the enzymes' hydrophobic active site. Perfluorinated denpols also stabilised curcumin more effectively, as shown by the fluorescence intensity, which was retained even in the absence of an enzyme. Additionally, HeLa cells exposed to the perfluorinated denpols up to a concentration of 100 g/mL for 72 hours showed almost no toxicity. The study concluded that the efficient drug release under physiological conditions and good encapsulation potential of these denpols show their potential to function as efficient DDS.¹⁰³

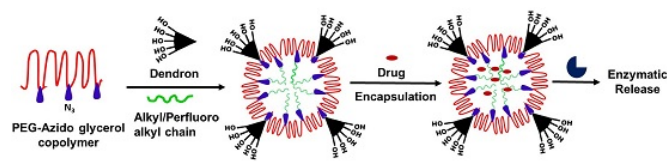


Figure 9. N435-mediated controlled release of hydrophobic drugs (red coloured) encapsulated in the denpols synthesized by click functionalization of PEG₁₀₀₀-co-azido glycerol base polymers with alkyl/fluoroalkyl chains and [G2.0]-OG dendrons. Reproduced from reference ¹⁰³. CC4.0.

N435 catalyzed PEG₆₀₀-co-azido-tri-glycerol polymers (Block copolymer 4)

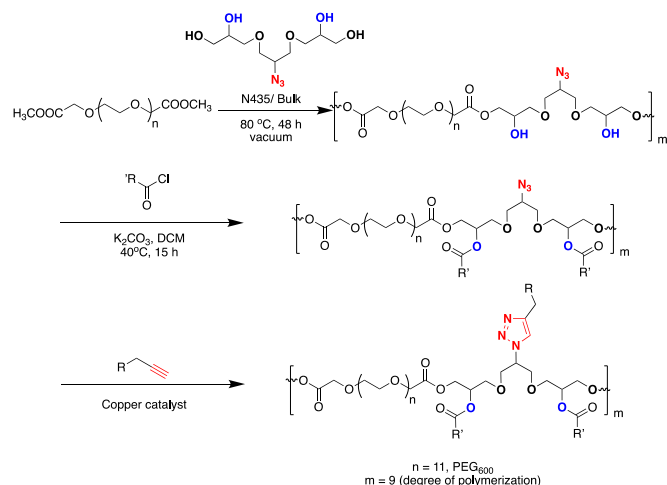
A series of supramolecular architectures with altered hydrophobic-hydrophilic balances were produced with the development in the synthesis of polyether-based PEG-co-azido-glycerol “clicked” denpols. These structures had high drug encapsulating efficiency and transport potentials, but to further fine-tune the supramolecular architecture another class of denpols were created by altering the base copolymer and adding azido-tri-glycerol as one of the monomers in the ongoing hunt for more precisely tuned structures. Azido-tri-glycerol is a versatile synthon which can be synthesized by several different methods reported in the literature.^{104–107} This monomer offers different functional groups (primary hydroxyl, secondary hydroxyl, and azide functional groups) for orthogonal chemistry.

Acylation with C-12 hydrophobic chains and orthogonal click functionalization with OG dendrons ([G1.0 and [G2.0] and hydrophobic chains (C-12)

Kumar *et al.*, bio-catalytically differentiated the primary and secondary hydroxyl groups of azido-tri-glycerol monomer and utilized the former for polymerization with PEG₆₀₀ diethyl ester generating PEG₆₀₀-co-azido-tri-glycerol polymers having orthogonal functionalities (secondary hydroxyl and azide functional groups) for post-functionalization to generate advanced polyether-based denpols (Scheme 6).¹⁰⁸ The backbone's secondary hydroxyl groups were available as an acylation site to refine the physicochemical features by attaching hydrophobic C-12 acyl chains (Table 1) as reported in the earlier work,⁹⁰ whereas by using the click-functionalization, the C-12 alkyl chains (Table 2) or [G1.0] and [G2.0]-OG dendrons (Table 3) were further grafted onto the copolymer *via* the azide group to generate the new generation of non-dendronized/dendronized polymers (Scheme 6, Table 5, entry 4.1).

The transport capacity was evaluated using hydrophilic Cy3, a dye which emits strong fluorescence in the visible spectrum (540–570 nm), and is known to aggregate in aqueous solutions.^{109,110} The dye was encapsulated in polymeric nanocarriers and subsequently evaluated for transport potential using UV absorption spectra and fluorescence emission spectra, which indicated a decreasing trend in transport potential with increasing hydrophilic content i.e. with an increase in OG grafting from [G1.0] to [G2.0]. The non-dendronized exclusively alkyl-grafted polymer had better transport capacity, while the acylated polymer without any click functionalization

i.e. with free pendant azide groups gave the best results with the highest transport capacity (19.15 mmol/mol). These results indicate that an appropriate hydrophobic core is essential for guest encapsulation depending on the nature of the guest molecule to achieve maximum loading.¹⁰⁸



Scheme 6. Synthesis of PEG-co-azido-tri-glycerol polymers and their acylation and click functionalization with various hydrophobic (Table 1 (acyl chlorides) and Table 2 (R groups)) and hydrophilic R groups (Table 3) to generate dendronized/non-dendronized polymers.

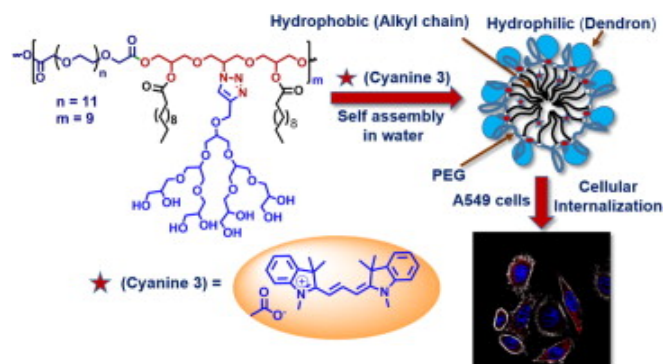


Figure 10. Schematic representation of denpol with C-12 acylation on secondary hydroxyl groups and [G2.0]-OG dendronization on azide group *via* click functionalization on azido-tri-glycerol monomer, Cyanine 3 dye encapsulation and self-assembly in aqueous solution and CLSM images of Cy3 internalization in A549 cells after an incubation period of 4 h. Cy3 loaded polymers appear red, nuclei are stained blue and cytoskeleton white. Reproduced from reference¹⁰⁸. Copyright 2015 Elsevier.

Subsequently, DLS and cryo-TEM studies were used to analyse the aggregation behaviour and size of the amphiphilic denpols in an aqueous media, with most of the polymers exhibiting stable micelles, except for exclusively C-12-functionalized non-dendronized polymer, which demonstrated the formation of vesicles of various sizes in addition to spherical micelles. The cytotoxicity evaluation of the denpols was conducted using A549 cell lines and dox as a reference drug with and without Cy3 loading. Both kinds were non-toxic up to a concentration of 100 $\mu\text{g/mL}$, while at 500 $\mu\text{g/mL}$ the denpols irrespective of Cy3 encapsulation were found to be less-toxic

than the partially and fully alkyl grafted non-dendronized polymers, which indicated that a fragile hydrophilic/hydrophobic balance is essential to minimize cytotoxicity. To investigate the internalisation of these synthetic denpols inside the cells, Cy3 was again utilised. According to CLSM and FACS measurements, the [G2.0] grafted denpols demonstrated greater cellular internalisation of Cy3 than the [G1.0] grafted denpols, which demonstrated insignificant uptake (Figure 10). These denpols' micellar size and CAC values have been compared to the analogues previously reported (Table 5, entries 2.1, 3.1 and 3.2).^{91–93} This study offered fresh perspectives on the imaging of cancer cell lines using polyether-based denpols.

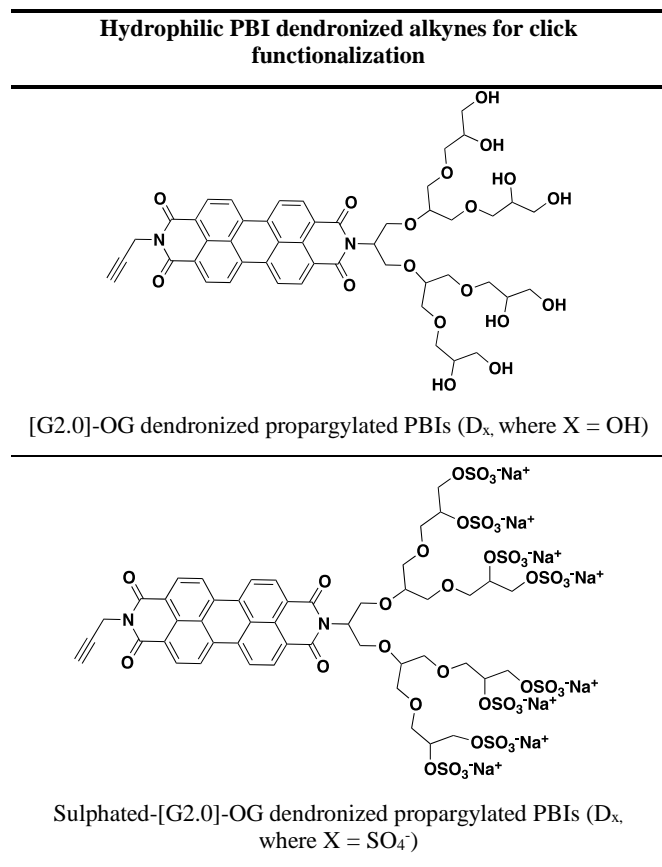
Acylation with C-11 terminal alkene hydrophobic chains and orthogonal click functionalization with OG dendrons ([G1.0 and [G2.0] and hydrophobic chains (C-12)

In a subsequent study by Kumar *et al.*, utilizing the same PEG₆₀₀-co-azido-tri-glycerol polymers, the post-polymeric functionalization was carried out with hydrophobic C-11 terminal alkenoyl chloride (Table 1) *via* acylation of secondary hydroxyl group and orthogonally by hydrophilic [G1.0] and [G2.0]-OG dendrons (Table 3) *via* highly efficient click chemistry to generate denpols (Scheme 6).¹¹¹ The idea behind the introduction of a terminal double bond in the hydrophobic side chains was to achieve better stabilization of micellar aggregates by π - π interactions among the peripheral double bonds. The same was observed by the reduced CAC values in the micromolar range (Table 5, entry 4.2)¹¹¹ of the denpols compared to the previous reports with similar denpols lacking the olefinic bonds in the hydrophobic side chains (Table 5, entry 4.1).¹⁰⁸

Additionally, the internalisation of Cy3 in these denpols was significantly reduced¹¹¹ than in denpol analogues without π -bonds,¹⁰⁸ and the plausible explanation relate to the stable aggregate formation achieved by π - π interactions, and preventing foreign guest molecules from entering easily into the hydrophobic core of the denpols. So, further development of a polymeric system with better capacity for encasing hydrophobic guest molecules and the ability to form stable aggregates was required.¹¹¹

Acylation with C-18 hydrophobic chains and orthogonal click functionalization with dendronized (hydroxylated/sulphated)-[G2.0]-OG PBIs

Bio-imaging studies were further reported by Huth *et al.*, by generating denpols (having PBI moieties) complexes with SWCNTs. PBIs (dye **D**) were chosen for this study as they have exceptional fluorescence characteristics, a long emission wavelength, and high photophysical and chemical stability, making them ideal for bio-imaging applications.^{112,113} They have been used in a variety of ways, such as fluorescent tags,^{114–117} membrane markers,^{118,119} or anti-inflammatory drugs.¹²⁰ PEG₆₀₀-co-azido-tri-glycerol-based block copolymers were functionalized with hydrophobic C-18 acyl chains (Table 1) *via* acylation procedure to generate non-dendronized polymers (P_{alkyl}) and further functionalized orthogonally *via* efficient click chemistry with [G2.0]-OG dendronized propargylated

Table 4. Different hydrophilic R groups used in Scheme 6 to generate PBI-dye labelled denpols (\mathbf{P}_x , where $X = \text{OH}/\text{SO}_4^-$)

PBIs (\mathbf{D}_x , $X = \text{OH}$, Table 4) or negatively charged sulphated-[G2.0]-OG dendronized propargylated PBIs (\mathbf{D}_x , $X = \text{SO}_4^-$, Table 4) to generate denpols (\mathbf{P}_x) (Scheme 6, Table 5, entry 4.3).¹²¹ Each part of this intricate system served certain

functions, such as the base copolymer solubilizes the toxic SWCNTs; the polyhydroxy glycerol dendron generates hydrophilicity and inhibits the quenching of the dye; the dendronized PBIs are fluorescent marker; and SWCNTs constitute the fundamental immobilisation framework. Further, a straightforward sulphation method was adopted to generate negatively charged denpols with the aim of further preventing fluorescence quenching agglomeration and enhancing receptor-mediated cellular uptake.¹²¹ Figure 11 schematically depicts the idealized wrapping of the polymers around the SWCNTs in a helical fashion after sonication in aqueous media.

Although SWCNTs have great potential for biomedical applications, still their utilisation is restricted due to their poor biocompatibility and cytotoxicity, which are brought on by their high aspect ratio and surface area.^{122–124} The use of commercially available surfactants (SDS/Triton X-100) promotes more decrease in the cytocompatibility of SWCNTs^{125,126} and thus, it was anticipated that the wrapping of the denpols around the SWCNTs (Figure 11) would be a better alternative than large amounts of high CMC surfactants. To investigate this, the $\mathbf{P}_{\text{alkyl}}$ -wrapped SWCNTs were studied for toxicity studies with HeLa cell lines and the results indicated a considerable increase in cell viability of polymer-wrapped SWCNTs compared to immaculate tubes from 66% to $\geq 98\%$, on the other hand, a decrease in viability was observed with surfactant-wrapped tubes by $\leq 20\%$. Compared to cells treated with surfactant-solubilized SWCNTs, which exhibit an elevated rate of cell death, cells treated with $\mathbf{P}_{\text{alkyl}}$ -wrapped SWCNTs were robust with good cell vitality.

Cellular uptake studies were performed *in vitro* on HeLa cells using the non-dendronized ($\mathbf{P}_{\text{alkyl}}$)/dendronized (\mathbf{P}_x)-SWCNT complexes. Qualitative and quantitative analysis was performed *via* CLSM (Figure 12A) and flow cytometry respectively (Figure 12B). The free dyes \mathbf{D}_x (neutral/charged i.e. $X = \text{OH}$ or

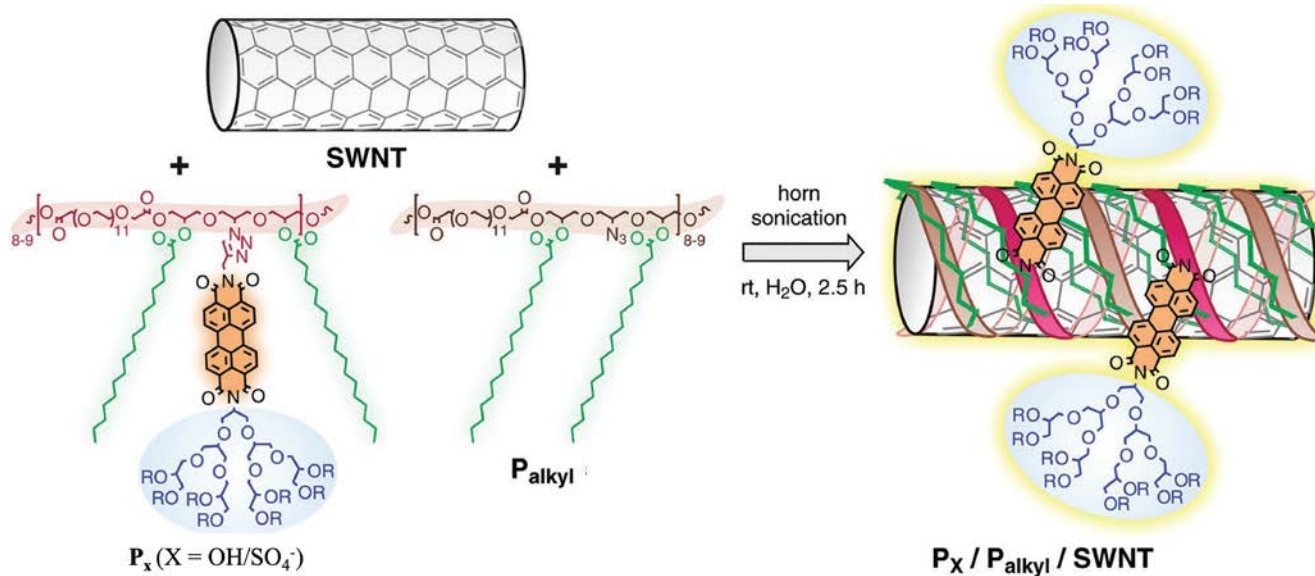


Figure 11. Schematic representation of polymer ($\mathbf{P}_x/\mathbf{P}_{\text{alkyl}}$)-SWCNT complexes formed by sonication in an aqueous solution ($X = \text{OH}/\text{SO}_4^-$) and their idealized wrapping around in helical patterns over the surface of nanotubes. Reproduced from reference ¹²¹. Copyright 2018 Wiley-VCH Verlag GmbH & Co. KGaA.

Table 5. Progression of polyether-based denpols using the versatile click chemistry and their applications for the delivery of active components.

S. No.	Polymers' side chain appendages to generate dendronized/non-dendronized polymers		Coupling strategy	CMC/CAC (M)	Molecular weight M_n (Da) by GPC	Applications of denpols	Ref.
	Hydrophobic R groups (% composition in final polymers)	Hydrophilic side chains					
Block copolymer 1	Poly(PEG₆₀₀-co-glycerol)						
1.1	C-5, C-7, C-9 acyl chlorides (100%)	-	Acylation reaction K ₂ CO ₃ , DCM, rt, 6 h	2.4 x 10 ⁻²	5.5 x 10 ³ 5.7 x 10 ³ 5.9 x 10 ³	Hydrophobic drug Vitamin E encapsulation	90
Block copolymer 2	Poly(PEG₆₀₀-co-azido-glycerol)						
2.1	C-18 (50-70%)	[G1.0], [G2.0]-OG dendrons (30-50%)	CuAAC: CuBr, DMF, rt, 24 h	2.0 x 10 ⁻⁵ - 2.94 x 10 ⁻⁵	2.9 x 10 ³ - 5.1 x 10 ³	Hydrophobic guest pyrene encapsulation and ANS binding studies	91
Block copolymer 3	Poly(PEG₁₀₀₀-co-azido-glycerol)						
3.1	C-12 and C-14 (50-100%)	[G1.0], [G2.0]-OG dendrons (30-50%)	CuAAC: CuSO ₄ .5H ₂ O, Sodium ascorbate, THF:H ₂ O (3:1), 40°C, 48-60 h	1.4 x 10 ⁻⁵ - 3.4 x 10 ⁻⁵	1.4 x 10 ³ - 8.8 x 10 ³	Hydrophobic dye Nile red encapsulation and cytotoxicity studies	92
3.2	C-18 (50-100%)	[G1.0], [G2.0]-OG hPG dendrons (0-50%)	CuAAC: CuSO ₄ .5H ₂ O, Sodium ascorbate, THF:H ₂ O (3:1), 40°C, 48-60 h	6.7 x 10 ⁻¹ - 34 x 10 ⁻⁶	1.1 x 10 ³ - 6.5 x 10 ³	Hydrophobic dye Nile red encapsulation by denpols and their significant uptake by QGP-1 cells, cytotoxicity profiles of denpols	93
3.3	Azobenzene (70%)	Without/with [G2.0]-OG dendrons (0-30%)	CuAAC: [Cu(PPh ₃) ₃]Br, DIPEA, DCM/DMF, rt, 48 h	1.07 x 10 ⁻⁵ - 1.66 x 10 ⁻⁵	4.3 x 10 ³ - 4.7 x 10 ³	Hydrophobic dye Curcumin and Nile red encapsulation by amphiphilic micelles and subsequent study of photoresponsive release of Nile Red.	98
3.4	Fluoro C-8 (50-70%)	[G2.0]-OG dendrons (30-50%)	CuAAC: [Cu(PPh ₃) ₃]Br, DIPEA, DCM/DMF, rt, 48 h	8.9 x 10 ⁻⁶ - 7.8 x 10 ⁻⁶	3.2 x 10 ³ - 4.1 x 10 ³	Solubilization and transport capacity evaluation of poorly water-soluble drugs curcumin and dexamethasone	103
	C-8 (50-70%)			1.2 x 10 ⁻⁵ - 4.5 x 10 ⁻⁵	1.4 x 10 ³ - 2.0 x 10 ³		
Block copolymer 4	Poly(PEG₆₀₀-co-azido-triglycerol)						
4.1	C-12 acyl chloride (R') (66%)	[G1.0] and [G2.0]-OG dendrons (33%)	Acylation: K ₂ CO ₃ , DCM, 35-40°C, 12 h CuAAC: CuSO ₄ .5H ₂ O, Sodium ascorbate, THF:H ₂ O (3:1), 50°C, 24 h	3.29 x 10 ⁻⁵ - 4.56 x 10 ⁻⁵	1.8 x 10 ³ - 10.4 x 10 ³	Cytotoxic evaluation of denpols in A549 cell lines. CLSM and FACS measurements demonstrated greater cellular internalisation of Cy3 by the [G2.0]-OG grafted denpols.	108
	C-12 acyl chloride (R') - acylation and/or C-12 (R) - click reaction (66-100%)						
4.2	C-11 terminal alkenoyl chloride (R') -acylation (66%)	[G1.0] and [G2.0]-OG dendrons (33%)	Acylation: K ₂ CO ₃ , DCM, 35-40°C, 12 h CuAAC: CuSO ₄ .5H ₂ O, Sodium ascorbate, THF:H ₂ O (3:1), 50°C, 24 h	1.9 x 10 ⁻⁵ - 4.23 x 10 ⁻⁶	8.0 x 10 ² - 15.7 x 10 ³	Non-toxicity of denpols upto a concentration of 500µg/mL in A549 cell lines and Cy3 encapsulation in sufficient amounts.	111
	C-11 terminal alkenoyl chloride (R') -acylation and/or C-12 (R) -click reaction (66-100%)						
4.3	C-18 acyl chloride	[G2.0]-OG PBI/[G2.0]-sulphated-OG dendronized PBI	Acylation: EDC, DMAP, DCM/DMF 0-35°C, 12 h CuAAC: Sodium ascorbate, CuSO ₄ .5H ₂ O, Cu Wire, DMF/H ₂ O, 50°C, 24 h	0.53 x 10 ⁻³ - 0.63 x 10 ⁻³	2.03 x 10 ³ - 54.5 x 10 ³	Water-soluble, fluorescent, and debundled SWCNT complexes were obtained with PBI grafted denpols that were found appropriate for bioimaging studies.	121

SO₄⁻) were not visible in the cells after a 4 h incubation period. In contrast, as evidenced by the fluorescent signals of the PBI dye, the dye-conjugated denpols (**P_x**) and the complex formed by **P_x/P_{alkyl}/SWCNT** demonstrated an active uptake. These results combined with the evidence that no signal was observed when free dye (**D_x**)/free dye-alkyl grafted polymer (**D_x/P_{alkyl}**) mixtures were used, concluded the necessity of covalent bonding of the dye with polymer backbone for cellular uptake.

Intracellular uptake studies of the complexes demonstrated an impressive performance of the denpol-SWCNT complex as a probe for bioimaging (Figure 12). The charged SWCNT-complex (sulphated denpols-complex) outperformed its non-charged analogue in biological and photophysical investigations in terms of cellular uptake, intracellular staining, and optical characteristics. Due to their nanosize dimensions, outstanding fluorescence, and great cytocompatibility, the denpol-SWCNT

complexes proved to be an important tool for fluorescent bioimaging with a wide range of applications.¹²¹

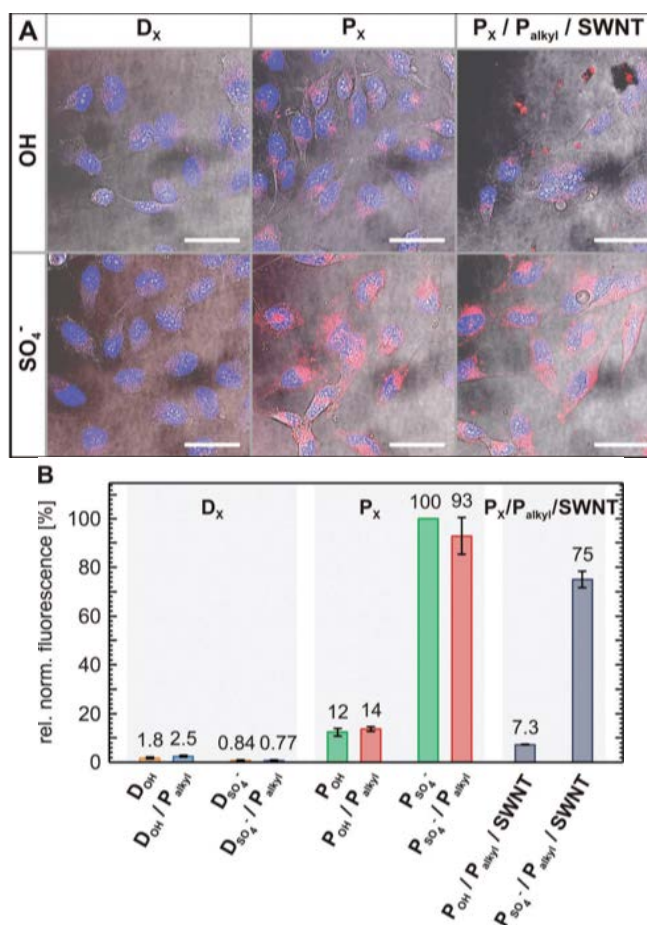


Figure 12. Cellular uptake studies *in vitro* on HeLa cells with free dye D_x ($X = OH/SO_4^-$), free dye-polymer mixtures (D_x/P_{alkyl}) and SWCNT complexes formed with PBI-dendronized/non-dendronized polymers ($P_x/P_{alkyl}/SWCNT$). **A)** After 4 hours of incubation, live-cell microscopy pictures of HeLa cells (cell nuclei stained blue) treated with the respective PBI-based compounds (stained red) are shown. Scale bar, 50 μM ; **B)** Analysis of flow cytometry data from HeLa cells treated with the above-mentioned compounds show that sulphated analogues outperform the hydroxylated denpols and SWCNT-denpol complexes in terms of uptake behaviour and staining efficiency. Reproduced from reference ¹²¹. Copyright 2018 Wiley-VCH Verlag GmbH & Co. KGaA

CONCLUSION

The versatility of “click chemistry” in various fields has already been comprehensively surveyed recently,¹²⁷ whereas herein another research area exploring this highly adaptable reaction has been reported. Despite its early stages of research, polyether-based dendronized multi-amphiphilic polymers have demonstrated remarkable potential as supramolecular self-assembled nano-transporters for the delivery of active pharmaceuticals, much work is still required to get over these dendronized nanocarriers’ constraints and explore them in clinical settings. Future research must also focus on strategies for bio-orthogonal click chemistry utilizing the many available end-groups for functionalization to attach molecular tags, drugs and dyes for *in vivo* studies. Further advancements in this field would open up new avenues for

enhancing the flexibility of denpols with polyether scaffolds and developing next-generation DDS.

ABBREVIATIONS

A549, Adenocarcinoma human alveolar basal epithelial cell lines; AAC, Azide-alkyne cycloaddition; ATRP, atom transfer radical polymerization; BARAC, Biarylazacyclooctynones; CAC, Critical Aggregation Concentration; CLSM, Confocal laser scanning microscopy; CMC, Critical Micelle Concentration; Cryo-TEM, Cryogenic Transmission Electron Microscopy; Cu(n), Copper with oxidation state n ($n=0, I, II$); CuAAC, Copper-catalyzed azide-alkyne cycloaddition; Cy3, Cyanine dye; DDS, Drug Delivery Systems; Denpols, Dendronized polymers; DIFO, Difluorocyclooctyne; DLS, Dynamic Light Scattering; Dox, Doxorubicin; FACS, Fluorescence-Assisted Cell Sorting; FDA, Food and Drug Administration; FT, Fourier Transform; [Gn.0], n^{th} Generation dendron ($n=1,2,3$ etc.); GPC, Gel Permeation Chromatography; hPG, hyperbranched polyglycerol; N435, Novozym 435; OG, Oligoglycerol; PBIs, Perylene bisimides; PEG, Polyethylene glycol; PG, Polyglycerol; ROMP, Ring-Opening Metathesis Polymerization; SDS, Sodium dodecyl sulphate; SLS, Static Light Scattering; SPAAC, Strain-promoted azide-alkyne cycloaddition; SWCNT, Single-Walled Carbon Nanotubes; TMTH, Tetramethylthiacycloheptyne; UV-vis spectroscopy, Ultraviolet-visible spectroscopy.

ACKNOWLEDGMENTS

The author acknowledges the help from Dr Shang Eun Park in certain specific areas of this article.

REFERENCES AND NOTES

- H.C. Kolb, M.G. Finn, K.B. Sharpless. Click Chemistry: Diverse Chemical Function from a Few Good Reactions. *Angewandte Chemie International Edition* **2001**, 40 (11), 2004–2021.
- P. Wu. The Nobel Prize in Chemistry 2022: Fulfilling Demanding Applications with Simple Reactions. *ACS Chem Biol* **2022**, 17 (11), 2959–2961.
- M. Boyce, S.A. Malaker, N.M. Riley, J.J. Kohler. The 2022 Nobel Prize in Chemistry—sweet! *Glycobiology* **2023**, 33 (3), 178–181.
- A.K. Agrahari, P. Bose, M.K. Jaiswal, et al. Cu(I)-Catalyzed Click Chemistry in Glycoscience and Their Diverse Applications. *Chem Rev* **2021**, 121 (13), 7638–7956.
- A. Michael. Ueber Die Einwirkung Von Diazobenzolimid Auf Acetylendicarbonsäuremethylester. *J. Prakt. Chem.* **1893**, 48, 94–95.
- R. Huisgen, G. Szeimies, L. Möbius. 1,3-Dipolare Cycloadditionen, XXXII. Kinetik der Additionen organischer Azide an CC-Mehrfachbindungen. *Chem Ber* **1967**, 100 (8), 2494–2507.
- M. Breugst, H. Reissig. The Huisgen Reaction: Milestones of the 1,3-Dipolar Cycloaddition. *Angewandte Chemie International Edition* **2020**, 59 (30), 12293–12307.
- R. Huisgen. 1,3-Dipolar Cycloadditions. Past and Future. *Angewandte Chemie International Edition in English* **1963**, 2 (10), 565–598.
- V. V. Rostovtsev, L.G. Green, V. V. Fokin, K.B. Sharpless. A Stepwise Huisgen Cycloaddition Process: Copper(I)-Catalyzed Regioselective “Ligation” of Azides and Terminal Alkynes. *Angewandte Chemie International Edition* **2002**, 41 (14), 2596–2599.
- C.W. Tornøe, C. Christensen, M. Meldal. Peptidotriazoles on Solid Phase: [1,2,3]-Triazoles by Regiospecific Copper(I)-Catalyzed 1,3-Dipolar Cycloadditions of Terminal Alkynes to Azides. *J Org Chem* **2002**, 67 (9), 3057–3064.
- M. Meldal, C.W. Tornøe. Cu-Catalyzed Azide–Alkyne Cycloaddition. *Chem Rev* **2008**, 108 (8), 2952–3015.
- S. Neumann, M. Biewend, S. Rana, W.H. Binder. The CuAAC: Principles, Homogeneous and Heterogeneous Catalysts, and Novel

- Developments and Applications. *Macromol Rapid Commun* **2020**, 41 (1), 1900359.
13. R. Berg, B.F. Straub. Advancements in the mechanistic understanding of the copper-catalyzed azide–alkyne cycloaddition. *Beilstein Journal of Organic Chemistry* **2013**, 9, 2715–2750.
 14. S. Díez-González, S.P. Nolan. [(NH₂)₂Cu]X Complexes as Efficient Catalysts for Azide–Alkyne Click Chemistry at Low Catalyst Loadings. *Angewandte Chemie International Edition* **2008**, 47 (46), 8881–8884.
 15. B.H. Lipshutz, B.A. Frieman, A.E. Tomaso. Copper-in-Charcoal (Cu/C): Heterogeneous, Copper-Catalyzed Asymmetric Hydrosilylations. *Angewandte Chemie International Edition* **2006**, 45 (8), 1259–1264.
 16. K.F. Suazo, K.-Y. Park, M.D. Distefano. A Not-So-Ancient Grease History: Click Chemistry and Protein Lipid Modifications. *Chem Rev* **2021**, 121 (12), 7178–7248.
 17. P. Thirumurugan, D. Matosiuk, K. Jozwiak. Click Chemistry for Drug Development and Diverse Chemical–Biology Applications. *Chem Rev* **2013**, 113 (7), 4905–4979.
 18. L. Taiariol, C. Chaix, C. Farre, E. Moreau. Click and Bioorthogonal Chemistry: The Future of Active Targeting of Nanoparticles for Nanomedicines. *Chem Rev* **2022**, 122 (1), 340–384.
 19. N.J. Agard, J.A. Prescher, C.R. Bertozzi. A strain-promoted [3 + 2] azide-alkyne cycloaddition for covalent modification of biomolecules in living systems. *J Am Chem Soc* **2004**, 126 (46), 15046–15047.
 20. J.M. Baskin, J.A. Prescher, S.T. Laughlin, et al. Copper-free click chemistry for dynamic in vivo imaging. *Proc Natl Acad Sci U S A* **2007**, 104 (43), 16793–16797.
 21. X. Ning, J. Guo, M.A. Wolfert, G.-J. Boons. Visualizing Metabolically Labeled Glycoconjugates of Living Cells by Copper-Free and Fast Huisgen Cycloadditions. *Angewandte Chemie* **2008**, 120 (12), 2285–2287.
 22. J. Dommerholt, S. Schmidt, R. Temming, et al. Readily Accessible Bicyclononynes for Bioorthogonal Labeling and Three-Dimensional Imaging of Living Cells. *Angewandte Chemie International Edition* **2010**, 49 (49), 9422–9425.
 23. J.C. Jewett, E.M. Sletten, C.R. Bertozzi. Rapid Cu-free click chemistry with readily synthesized biarylazacyclooctynones. *J Am Chem Soc* **2010**, 132 (11), 3688–3690.
 24. G. de Almeida, E.M. Sletten, H. Nakamura, K.K. Palaniappan, C.R. Bertozzi. Thiacycloalkynes for Copper-Free Click Chemistry. *Angewandte Chemie* **2012**, 124 (10), 2493–2497.
 25. X. Yang, S. Wang, Y. Yan, et al. Well-defined dibenzocyclooctyne end functionalized polymers from atom transfer radical polymerization. *Polymer (Guildf)* **2014**, 55 (5), 1128–1135.
 26. D. Wu, K. Yang, Z. Zhang, et al. Metal-free bioorthogonal click chemistry in cancer theranostics. *Chem Soc Rev* **2022**, 51 (4), 1336–1376.
 27. S. Jatav, N. Pandey, P. Dwivedi, et al. Synthesis of deoxy-Andrographolide Triazolyl Glycoconjugates for the Treatment of Alzheimer's Disease. *ACS Chem Neurosci* **2022**, 13 (23), 3271–3280.
 28. N. Pandey, Jyoti, M. Singh, et al. Click chemistry inspired synthesis of andrographolide triazolyl conjugates for effective fluorescent sensing of ferric ions. <https://doi.org/10.1080/14786419.2021.2013837> **2021**, 36 (21), 5438–5448.
 29. N. Pandey, P. Dwivedi, Jyoti, et al. Click Chemistry Inspired Synthesis of Hydroxyanthracene Triazolyl Glycoconjugates. *ACS Omega* **2022**, 7 (42), 37112–37121.
 30. Z. Geng, J.J. Shin, Y. Xi, C.J. Hawker. Click chemistry strategies for the accelerated synthesis of functional macromolecules. *Journal of Polymer Science* **2021**, 59 (11), 963–1042.
 31. J. Kaur, M. Saxena, N. Rishi. An Overview of Recent Advances in Biomedical Applications of Click Chemistry. *Bioconjug Chem* **2021**, 32 (8), 1455–1471.
 32. N.Z. Fantoni, A.H. El-Sagheer, T. Brown. A Hitchhiker's Guide to Click-Chemistry with Nucleic Acids. *Chem Rev* **2021**, 121 (12), 7122–7154.
 33. D. Pereira, M. Pinto, M. Correia-da-Silva, H. Cidade. Recent Advances in Bioactive Flavonoid Hybrids Linked by 1,2,3-Triazole Ring Obtained by Click Chemistry. *Molecules* **2021**, 27 (1), 230.
 34. X. Li, Y. Xiong. Application of “Click” Chemistry in Biomedical Hydrogels. *ACS Omega* **2022**, 7 (42), 36918–36928.
 35. V.K. Tiwari, B.B. Mishra, K.B. Mishra, et al. Cu-Catalyzed Click Reaction in Carbohydrate Chemistry. *Chem Rev* **2016**, 116 (5), 3086–3240.
 36. Sengupta P, Dutta S, Chhikara BS. Bioorthogonal chemistry in the reproductive medicine. *Chemical Biology Letters* **2023**, 10 (3), 545.
 37. A. Kolate, D. Baradia, S. Patil, et al. PEG — A versatile conjugating ligand for drugs and drug delivery systems. *Journal of Controlled Release* **2014**, 192, 67–81.
 38. K. Knop, R. Hoogenboom, D. Fischer, U.S. Schubert. Poly(ethylene glycol) in Drug Delivery: Pros and Cons as Well as Potential Alternatives. *Angewandte Chemie International Edition* **2010**, 49 (36), 6288–6308.
 39. A.A. D'souza, R. Shegokar. Polyethylene glycol (PEG): a versatile polymer for pharmaceutical applications. *Expert Opin Drug Deliv* **2016**, 13 (9), 1257–1275.
 40. S. Gupta, R. Tyagi, V.S. Parmar, S.K. Sharma, R. Haag. Polyether based amphiphiles for delivery of active components. *Polymer (Guildf)* **2012**, 53 (15), 3053–3078.
 41. M. Calderín, M.A. Quadir, S.K. Sharma, R. Haag. Dendritic Polyglycerols for Biomedical Applications. *Advanced Materials* **2010**, 22 (2), 190–218.
 42. D. Wilms, S.-E. Stürba, H. Frey. Hyperbranched Polyglycerols: From the Controlled Synthesis of Biocompatible Polyether Polyols to Multipurpose Applications. *Acc Chem Res* **2010**, 43 (1), 129–141.
 43. J. Khandare, M. Calderón, N.M. Dagia, R. Haag. Multifunctional dendritic polymers in nanomedicine: opportunities and challenges. *Chem. Soc. Rev.* **2012**, 41 (7), 2824–2848.
 44. B.N.S. Thota, L.H. Uner, R. Haag. Supramolecular Architectures of Dendritic Amphiphiles in Water. *Chem Rev* **2016**, 116 (4), 2079–2102.
 45. P. Pouyan, M. Cherri, R. Haag. Polyglycerols as Multi-Functional Platforms: Synthesis and Biomedical Applications. *Polymers (Basel)* **2022**, 14 (13), 2684.
 46. H. Dau, G.R. Jones, E. Tsogtgerel, et al. Linear Block Copolymer Synthesis. *Chem Rev* **2022**, 122 (18), 14471–14553.
 47. B. Helms, J.L. Mynar, C.J. Hawker, J.M.J. Fréchet. Dendronized Linear Polymers via “Click Chemistry.” *J Am Chem Soc* **2004**, 126 (46), 15020–15021.
 48. X. Liu, W. Lin, D. Astruc, H. Gu. Syntheses and applications of dendronized polymers. *Prog Polym Sci* **2019**, 96, 43–105.
 49. X. Liu, L. Wang, I. Gitsov. Novel Amphiphilic Dendronized Copolymers Formed by Enzyme-Mediated “Green” Polymerization. *Biomacromolecules* **2021**, 22 (4), 1706–1720.
 50. C.J. Hawker, J.M.J. Fréchet. Preparation of polymers with controlled molecular architecture. A new convergent approach to dendritic macromolecules. *J Am Chem Soc* **1990**, 112 (21), 7638–7647.
 51. D.A. Tomalia, A.M. Naylor, W.A. Goddard. Starburst Dendrimers: Molecular-Level Control of Size, Shape, Surface Chemistry, Topology, and Flexibility from Atoms to Macroscopic Matter. *Angewandte Chemie International Edition in English* **1990**, 29 (2), 138–175.
 52. V. Percec, C.H. Ahn, W.D. Cho, et al. Visualizable cylindrical macromolecules with controlled stiffness from backbones containing libraries of self-assembling dendritic side groups. *J Am Chem Soc* **1998**, 120 (34), 8619–8631.
 53. S. Förster, I. Neubert, A.D. Schlüter, P. Lindner. How dendrons stiffen polymer chains: A SANS study. *Macromolecules* **1999**, 32 (12), 4043–4049.

54. N. Ouali, S. Méry, A. Skoulios, L. Noirez. Backbone Stretching of Wormlike Carbosilane Dendrimers. *Macromolecules* **2000**, 33 (16), 6185–6193.
55. J. Roeser, F. Moingeon, B. Heinrich, et al. Dendronized polymers with peripheral oligo(ethylene oxide) chains: Thermoresponsive behavior and shape anisotropy in solution. *Macromolecules* **2011**, 44 (22), 8925–8935.
56. A. Zhang, L. Shu, Z. Bo, A.D. Schlüter. Dendronized Polymers: Recent Progress in Synthesis. *Macromol Chem Phys* **2003**, 204 (2), 328–339.
57. H. Frauenrath. Dendronized polymers - Building a new bridge from molecules to nanoscopic objects. *Progress in Polymer Science (Oxford)* **2005**, 30 (3–4), 325–384.
58. J.L. Mynar, T.-L. Choi, M. Yoshida, et al. Doubly-dendronized linear polymers. *Chemical Communications* **2005**, No. 41, 5169.
59. P. Perdih, A. Kržan, E. Žagar. Synthesis of Dendronized Poly(l-Glutamate) via Azide-Alkyne Click Chemistry. *Materials (Basel)* **2016**, 9 (4).
60. M. Tonga, G. Yesilbag Tonga, G. Seber, O. Gok, A. Sanyal. Dendronized polystyrene via orthogonal double-click reactions. *J Polym Sci A Polym Chem* **2013**, 51 (23), 5029–5037.
61. B. Karakaya, W. Claussen, K. Gessler, W. Saenger, A.D. Schlüter. Toward dendrimers with cylindrical shape in solution. *J Am Chem Soc* **1997**, 119 (14), 3296–3301.
62. B. Helms, J.L. Mynar, C.J. Hawker, J.M.J. Fréchet. Dendronized linear polymers via “click chemistry.” *J Am Chem Soc* **2004**, 126 (46), 15020–15021.
63. A. Desai, N. Atkinson, F. Rivera, et al. Hybrid dendritic–linear graft copolymers: Steric considerations in “coupling to” approach. *J Polym Sci A Polym Chem* **2000**, 38 (6), 1033–1044.
64. H. Zeng, H.C. Little, T.N. Tiambeng, G.A. Williams, Z. Guan. Multifunctional dendronized peptide polymer platform for safe and effective siRNA delivery. *J Am Chem Soc* **2013**, 135 (13), 4962–4965.
65. B.A. Laurent, S.M. Grayson. Synthesis of cyclic dendronized polymers via divergent “graft- from” and convergent click “graft-to” routes: Preparation of modular toroidal macromolecules. *J Am Chem Soc* **2011**, 133 (34), 13421–13429.
66. L. Shu, A.D. Schlüter, C. Ecker, N. Severin, J.P. Rabe. Extremely Long Dendronized Polymers: Synthesis, Quantification of Structure Perfection, Individualization, and SFM Manipulation. *Angewandte Chemie International Edition* **2001**, 40 (24), 4666–4669.
67. E.H. Kang, I.S. Lee, T.L. Choi. Ultrafast cyclopolymerization for polyene synthesis: Living polymerization to dendronized polymers. *J Am Chem Soc* **2011**, 133 (31), 11904–11907.
68. P. Sonar, H. Benmansour, T. Geiger, A.D. Schlüter. Thiophene-based dendronized macromonomers and polymers. *Polymer (Guildf)* **2007**, 48 (17), 4996–5004.
69. E. Kasëmi, W. Zhuang, J.P. Rabe, et al. Synthesis of an anionically chargeable, high-molar-mass, second-generation dendronized polymer and the observation of branching by scanning force microscopy. *J Am Chem Soc* **2006**, 128 (15), 5091–5099.
70. D. Marsitzky, R. Vestberg, P. Blainey, et al. Self-Encapsulation of Poly-2,7-fluorenes in a Dendrimer Matrix. *J Am Chem Soc* **2001**, 123 (29), 6965–6972.
71. B.M. Rosen, C.J. Wilson, D.A. Wilson, et al. Dendron-mediated self-assembly, disassembly, and self-organization of complex systems. *Chem Rev* **2009**, 109 (11), 6275–6540.
72. E. Kasëmi, W. Zhuang, J.P. Rabe, et al. Synthesis of an anionically chargeable, high-molar-mass, second-generation dendronized polymer and the observation of branching by scanning force microscopy. *J Am Chem Soc* **2006**, 128 (15), 5091–5099.
73. V. Percec, J. Heck, D. Tomazos, et al. Self-assembly of taper-shaped monoesters of oligo(ethylene oxide) with 3,4,5-tris(p-dodecyloxybenzyloxy)benzoic acid and of their polymethacrylates into tubular supramolecular architectures displaying a columnar mesophase. *J Chem Soc Perkin 1* **1993**, No. 22, 2799–2811.
74. V. Percec, J. Heck, M. Lee, G. Ungar, A. Alvarez-Castillo. Poly{2-vinylxyethyl 3,4,5-tris[4-(n-dodecanyloxy)benzyloxy]benzoate}: a self-assembled supramolecular polymer similar to tobacco mosaic virus. *J Mater Chem* **1992**, 2 (10), 1033–1039.
75. M.N. Holerca, D. Sahoo, B.E. Partridge, et al. Dendronized Poly(2-oxazoline) Displays within only Five Monomer Repeat Units Liquid Quasicrystal, A15 and σ Frank-Kasper Phases. *J Am Chem Soc* **2018**, 140 (49), 16941–16947.
76. M. Malkoch, A. Carlmark, A. Woldegiorgis, A. Hult, E.E. Malmström. Dendronized Aliphatic Polymers by a Combination of ATRP and Divergent Growth. *Macromolecules* **2003**, 37 (2), 322–329.
77. K.O. Kim, T.L. Choi. Synthesis of rod-like dendronized polymers containing G4 and G5 ester dendrons via macromonomer approach by living ROMP. *ACS Macro Lett* **2012**, 1 (4), 445–448.
78. K.O. Kim, T.L. Choi. Synthesis of dendronized polymers via macromonomer approach by living ROMP and their characterization: From rod-like homopolymers to block and gradient copolymers. *Macromolecules* **2013**, 46 (15), 5905–5914.
79. A. -D Schlüter, G. Wegner. Palladium and nickel catalyzed polycondensation - The key to structurally defined polyarylenes and other aromatic polymers. *Acta Polymerica* **1993**, 44 (2), 59–69.
80. Z. Bao, K.R. Amundson, A.J. Lovinger. Poly(phenylenevinylene)s with dendritic side chains: Synthesis, self-ordering, and liquid crystalline properties. *Macromolecules* **1998**, 31 (24), 8647–8649.
81. A. Kumar, A. Khan, S. Malhotra, et al. Synthesis of macromolecular systems via lipase catalyzed biocatalytic reactions: applications and future perspectives. *Chem Soc Rev* **2016**, 45 (24), 6855–6887.
82. S. Kobayashi, H. Uyama, S. Kimura. Enzymatic polymerization. *Chem Rev* **2001**, 101 (12), 3793–3818.
83. R.A. Gross, A. Kumar, B. Kalra. Polymer synthesis by in vitro enzyme catalysis. *Chem Rev* **2001**, 101 (7), 2097–2124.
84. J. ichi Kadokawa, S. Kobayashi. Polymer synthesis by enzymatic catalysis. *Curr Opin Chem Biol* **2010**, 14 (2), 145–153.
85. F. Hollmann, I.W.C.E. Arends. Enzyme Initiated Radical Polymerizations. *Polymers (Basel)* **2012**, 4 (1), 759–793.
86. J. Zhang, H. Shi, D. Wu, et al. Recent developments in lipase-catalyzed synthesis of polymeric materials. *Process Biochemistry* **2014**, 49 (5), 797–806.
87. Y. Yang, J. Zhang, D. Wu, et al. Chemoenzymatic synthesis of polymeric materials using lipases as catalysts: A review. *Biotechnol Adv* **2014**, 32 (3), 642–651.
88. B. Parshad, M. Kumari, V. Khatri, et al. Enzymatic synthesis of glycerol, azido-glycerol and azido-triglycerol based amphiphilic copolymers and their relevance as nanocarriers: A review. *Eur Polym J* **2021**, 158, 110690.
89. M.A. Qadir, R. Haag. Biofunctional nanosystems based on dendritic polymers. *Journal of Controlled Release* **2012**, 161 (2), 484–495.
90. S. Gupta, M.K. Pandey, K. Levon, et al. Biocatalytic Approach for the Synthesis of Glycerol-Based Macroamphiphiles and their Self-Assembly to Micellar Nanotransporters. *Macromol Chem Phys* **2010**, 211 (2), 239–244.
91. S. Gupta, B. Schade, S. Kumar, et al. Non-ionic Dendronized Multiamphiphilic Polymers as Nanocarriers for Biomedical Applications. *Small* **2013**, 9 (6), 894–904.
92. M. Kumari, A.K. Singh, S. Kumar, et al. Synthesis of amphiphilic dendronized polymers to study their self-assembly and transport behavior. *Polym Adv Technol* **2014**, 25 (11), 1208–1215.
93. M. Kumari, S. Gupta, K. Achazi, et al. Dendronized Multifunctional Amphiphilic Polymers as Efficient Nanocarriers for Biomedical Applications. *Macromol Rapid Commun* **2015**, 36 (2), 254–261.
94. X. Xue, J. Zhu, Z. Zhang, et al. Soluble Main-Chain Azobenzene Polymers via Thermal 1,3-Dipolar Cycloaddition: Preparation and Photoresponsive Behavior. *Macromolecules* **2010**, 43 (6), 2704–2712.

95. X. Kang, J. Zhao, H. Li, S. He. Synthesis of a main-chain liquid crystalline azo-polymer via “click” chemistry. *Colloid Polym Sci* **2013**, 291 (9), 2245–2251.
96. Z. Li, Y. Zhang, L. Zhu, T. Shen, H. Zhang. Efficient synthesis of photoresponsive azobenzene-containing side-chain liquid crystalline polymers with high molecular weights by click chemistry. *Polym Chem* **2010**, 1 (9), 1501.
97. K. Watari, H. Kouzai. Synthesis and Properties of Substituted Polyacetylenes Containing a Photosensitive Moiety in the Side Group. *Polym J* **2006**, 38 (3), 298–301.
98. M. Kumari, M. Billamboz, E. Leonard, et al. Self-assembly, photoresponsive behavior and transport potential of azobenzene grafted dendronized polymeric amphiphiles. *RSC Adv* **2015**, 5 (60), 48301–48310.
99. M.P. Krafft, J.G. Riess. Selected physicochemical aspects of poly- and perfluoroalkylated substances relevant to performance, environment and sustainability—Part one. *Chemosphere* **2015**, 129, 4–19.
100. M.P. Krafft, J.G. Riess. Highly fluorinated amphiphiles and colloidal systems, and their applications in the biomedical field. A contribution. *Biochimie* **1998**, 80 (5–6), 489–514.
101. M.K. Pandey, R. Tyagi, K. Yang, et al. Design and synthesis of perfluorinated amphiphilic copolymers: Smart nanomicelles for theranostic applications. *Polymer (Guildf)* **2011**, 52 (21), 4727–4735.
102. M. Pierre, K. Systè, O. Fluorés, F. Thérapeutiques, M.P. Krafft Is Director. Highly fluorinated compounds induce phase separation in, and nanostructure of liquid media. Possible impact on, and use in chemical reactivity control. *J Polym Sci A Polym Chem* **2006**, 44 (14), 4251–4258.
103. B. Parshad, M. Kumari, K. Achazi, et al. Chemo-Enzymatic Synthesis of Perfluoroalkyl-Functionalized Dendronized Polymers as Cyto-Compatible Nanocarriers for Drug Delivery Applications. *Polymers (Basel)* **2016**, 8 (8), 311.
104. M. Wyszogrodzka, K. Möws, S. Kamlage, et al. New Approaches Towards Monoamino Polyglycerol Dendrons and Dendritic Triblock Amphiphiles. *European J Org Chem* **2008**, 2008 (1), 53–63.
105. M. Wyszogrodzka, R. Haag. A Convergent Approach to Biocompatible Polyglycerol “Click” Dendrons for the Synthesis of Modular Core–Shell Architectures and Their Transport Behavior. *Chemistry – A European Journal* **2008**, 14 (30), 9202–9214.
106. A. Mittal, A.K. Singh, A. Kumar, et al. Fabrication of oligo-glycerol based hydrolase responsive amphiphilic nanocarriers. *Polym Adv Technol* **2020**, 31 (6), 1208–1217.
107. S. Kumar, K. Ludwig, B. Schade, et al. Introducing Chirality into Nonionic Dendritic Amphiphiles and Studying Their Supramolecular Assembly. *Chem. – A Eur. J.* **2016**, 22 (16), 5629–5636.
108. S. Kumar, K. Achazi, C. Böttcher, et al. Encapsulation and cellular internalization of cyanine dye using amphiphilic dendronized polymers. *Eur Polym J* **2015**, 69, 416–428.
109. S. Kirstein, S. Daehne. J-aggregates of amphiphilic cyanine dyes: Self-organization of artificial light harvesting complexes. *Int. J. Photoenergy* **2006**, 2006.
110. W. West, S. Pearce. The dimeric state of cyanine dyes. *Journal of Physical Chemistry* **1965**, 69 (6), 1894–1903.
111. S. Kumar, K. Achazi, K. Licha, et al. Chemo-enzymatic synthesis of dendronized polymers for cyanine dye encapsulation. *Advances in Polymer Technology* **2018**, 37 (6), 1797–1805.
112. T. Weil, T. Vosch, J. Hofkens, K. Peneva, K. Müllen. The Rylene Colorant Family—Tailored Nanoemitters for Photonics Research and Applications. *Angewandte Chemie International Edition* **2010**, 49 (48), 9068–9093.
113. M. Sun, K. Müllen, M. Yin. Water-soluble perylenediimides: design concepts and biological applications. *Chem Soc Rev* **2016**, 45 (6), 1513–1528.
114. K. Peneva, G. Mihov, F. Nolde, et al. Water-Soluble Monofunctional Perylene and Terrylene Dyes: Powerful Labels for Single-Enzyme Tracking. *Angewandte Chemie* **2008**, 120 (18), 3420–3423.
115. K. Huth, T. Heek, K. Achazi, et al. Noncharged and Charged Monodendronised Perylene Bisimides as Highly Fluorescent Labels and their Bioconjugates. *Chem. – A Eur. J.* **2017**, 23 (20), 4849–62.
116. J. Qu, C. Kohl, M. Pottek, K. Müllen. Ionic Perylenetetracarboxydiimides: Highly Fluorescent and Water-Soluble Dyes for Biolabeling. *Angew. Chem. Int. Ed.* **2004**, 43 (12), 1528–31.
117. K. Peneva, G. Mihov, A. Herrmann, et al. Exploiting the nitrilotriacetic acid moiety for biolabeling with ultrastable perylene dyes. *J Am Chem Soc* **2008**, 130 (16), 5398–5399.
118. T. Heek, J. Nikolaus, R. Schwarzer, et al. An amphiphilic perylene imido diester for selective cellular imaging. *Bioconjug Chem* **2013**, 24 (2), 153–158.
119. C. Jung, B.K. Müller, D.C. Lamb, et al. A new photostable terrylene diimide dye for applications in single molecule studies and membrane labeling. *J Am Chem Soc* **2006**, 128 (15), 5283–5291.
120. T. Heek, C. Kühne, H. Depner, et al. Synthesis, Photophysical, and Biological Evaluation of Sulfated Polyglycerol Dendronized Perylenebisimides (PBIs)- A Promising Platform for Anti-Inflammatory Theranostic Agents? *Bioconjug Chem* **2016**, 27 (3), 727–736.
121. K. Huth, M. Glaeske, K. Achazi, et al. Fluorescent Polymer-Single-Walled Carbon Nanotube Complexes with Charged and Noncharged Dendronized Perylene Bisimides for Bioimaging Studies. *Small* **2018**, 14 (28), 1800796.
122. Z. Sun, Z. Liu, J. Meng, et al. Carbon Nanotubes Enhance Cytotoxicity Mediated by Human Lymphocytes In Vitro. *PLoS One* **2011**, 6 (6), e21073.
123. J. Wang, P. Sun, Y. Bao, J. Liu, L. An. Cytotoxicity of single-walled carbon nanotubes on PC12 cells. *Toxicology in Vitro* **2011**, 25 (1), 242–250.
124. X. Shi, B. Sitharaman, Q.P. Pham, et al. In vitro cytotoxicity of single-walled carbon nanotube/biodegradable polymer nanocomposites. *J Biomed Mater Res A* **2008**, 86A (3), 813–823.
125. H. Wang, W. Zhou, D.L. Ho, et al. Dispersing single-walled carbon nanotubes with surfactants: A small angle neutron scattering study. *Nano Lett* **2004**, 4 (9), 1789–1793.
126. Z. Liu, S. Tabakman, K. Welscher, H. Dai. Carbon nanotubes in biology and medicine: In vitro and in vivo detection, imaging and drug delivery. *Nano Res* **2009**, 2 (2), 85–120.
127. N.K. Devaraj, M.G. Finn. Introduction: Click Chemistry. *Chem Rev* **2021**, 121 (12), 6697–6698.

AUTHOR'S BIOGRAPHY



Shilpi Gupta received her PhD degree in organic synthesis at the University of Delhi, India in 2011 under the guidance of Prof. Sunil K Sharma. After postdoctoral work with Prof. Rainer Haag at Free University Berlin, Germany, she joined the Department of Chemistry Hindu College, Sonipat as an Assistant Professor in 2013. She is recipient of several meritorious awards for excellence in academic performance, and research grants, including the 2016 prestigious Indo-US Postdoctoral Fellowship grant, supported by SERB and IUSSTF, India for research work conducted at CUSP, Irvine, California, USA. Her current research interests are in developing novel biocompatible drug delivery systems for delivering aboriginal drugs into biological environment while retaining their beneficial properties but eliminating the pathways leading to their biodegradation.